

Helium ($\gamma, 2e$) triple differential cross sections at an excess energy of 60 eV.

C. Dawson^(a), S. Cvejanoviæ^{(a)†}, D. P. Seccombe^(a), T. J. Reddish^(a),
F. Maulbetsch^(a), A. Huetz^(b), J. Mazeau^(b), and A. S. Kheifets^(c)

(a) Physics Department, Newcastle University, Newcastle-upon-Tyne, NE1 7RU, UK

(b) Laboratoire de Spectroscopie Atomique et Ionique, Université Paris-Sud,
Bat. 350, 91405, Orsay Cedex, France

(c) Research School of Physical Sciences and Engineering, Australian National University,
Canberra, ACT 0200, Australia

Abstract. ($\gamma, 2e$) triple differential cross sections (TDCS) are presented for helium at 60 eV above the photodouble ionisation threshold with energy sharing ratios ($R = E_2/E_1$) for the two ejected electrons of $R = 1, 5$ and 11. The measurements were taken using a toroidal spectrometer and linearly polarised light from an undulator beamline (SU6) at the Super-ACO synchrotron. Good agreement is found with TDCSs obtained by the CCC method and by the length gauge of 3C theory.

Photodouble ionisation (PDI) of helium has been the topic of a large number of experimental and theoretical investigations, which have recently been reviewed by Briggs and Schmidt (2000). This process is of fundamental interest because it results in a ‘structureless’ ion and two free electrons that mutually interact *via* the long-range Coulomb force. Thus, by using helium as the target, this particular aspect of electron correlation can be probed in isolation from other indirect PDI phenomena. Triple differential cross section (TDCS) measurements using linearly polarised light, summarised in table 1, have been made from the PDI threshold (79 eV) up to energies of 131.9 eV. Circular dichroism (CD) has also been investigated for a range of unequal energy-sharing conditions (Viefhaus *et al* 1996b, Mergel *et al* 1998, Soejima *et al* 1999, Kheifets *et al* 1999, Achler *et al* 2001). The results of all these experimental studies have been compared with TDCS calculations using a variety of theoretical methods. The early calculations included the three Coulomb wavefunction (3C) (Maulbetsch and Briggs 1993a, b, 1994), the two screened Coulomb wavefunction (2SC) (Proulx and Shakeshaft 1993, Pont and Shakeshaft 1995) and wavepacket propagation (Kazansky and Ostrovsky 1994, 1995) treatments. More recent advances have led to the development of, for example, the converged close coupling (CCC) (Kheifets and Bray 1998a,b,c,d, 2000), the time dependent close coupling (Pindzola and Robicheaux 2000), and the hyperspherical R -matrix with semiclassical outgoing waves (HRM-SOW) (Malegat *et al* 1999a,b,c, 2000) methods. The 3C and 2SC theories are compared in Maulbetsch *et al* (1995) and Pont *et al* (1996). In the latter paper there were shown to be significant discrepancies between theory and the experiments of Lablanquie *et al* (1995) for a range of energy-sharing conditions. More recently, helium TDCSs obtained using the HRM-SOW method (Malegat *et al* 2000) are in excellent agreement with those from 2SC and compare well with the data of Mazeau *et al* (1996). This development is encouraging as HRM-SOW is significantly less intensive on computing power than other approaches.

Whilst some of the latest theories based on numerical methods are extremely good at reproducing experimental data, they do not necessarily provide a simple framework for

[†] Current Address: Fritz-Haber-Institut der Max-Planck-Gesellschaft, Faradayweg 4-6, D-14195, Berlin, Germany.

understanding the underlying physical processes. An early theoretical contribution in this area was made by Huetz *et al* (1991) (later extended by Lablanquie *et al* 1995 and Malegat *et al* 1997a,b) who showed that for linearly polarised radiation, the helium TDCS can be expressed exactly as:

$$TDCS = \left| a_g (\cos \mathbf{q}_1 + \cos \mathbf{q}_2) + a_u (\cos \mathbf{q}_1 - \cos \mathbf{q}_2) \right|^2 \quad (1)$$

where \mathbf{q}_1 and \mathbf{q}_2 are the angles of the emitted electrons with respect to the electric field vector and a_g and a_u are the gerade and ungerade amplitudes. These two amplitudes are symmetric and antisymmetric respectively for interchange of the two electrons and depend on their energies (E_1 and E_2) and their mutual angle (\mathbf{q}_{12}). In the absence of circularly polarised light ($S_3 = 0$), and in a frame chosen to ensure $S_2 = 0$, the coplanar TDCS can be written as:

$$TDCS = PI + S_1 LD \quad (2)$$

$$PI = (1 + \cos(\mathbf{q}_2 - \mathbf{q}_1)) |a_g|^2 + (1 - \cos(\mathbf{q}_2 - \mathbf{q}_1)) |a_u|^2 \quad (3)$$

$$LD = |a_g|^2 [\cos^2 \mathbf{q}_1 - \sin^2 \mathbf{q}_2 + \cos(\mathbf{q}_1 + \mathbf{q}_2)] + |a_u|^2 [\cos^2 \mathbf{q}_1 - \sin^2 \mathbf{q}_2 - \cos(\mathbf{q}_1 + \mathbf{q}_2)] + 2 |a_g| |a_u| (\sin^2 \mathbf{q}_2 - \sin^2 \mathbf{q}_1) \cos \mathbf{f} \quad (4)$$

where S_1 , S_2 and S_3 are the Stokes parameters and PI and LD are the polarisation insensitive and linear dichroism contributions to the total cross section. The quantity \mathbf{f} denotes the phase angle between the gerade and ungerade amplitudes and formally depends on E_1 , E_2 and \mathbf{q}_{12} . TDCS measurements for a range of experimental conditions can be compared by parametrising equations (1) or (2) with suitable functions for a_g and a_u . It is anticipated that *ab initio* theories will soon evaluate these amplitudes directly.

In this letter we present TDCSs measured with an excess energy, E , of 60 eV ($h\nu = 139$ eV) for three energy sharing conditions ($R = E_2/E_1 = 1, 5$ and 11) along with those calculated by the 3C and CCC methods. This work is essentially an extension to higher E and R of our study at 40 eV ($h\nu = 119$ eV) above threshold (Cvejanoviæ *et al* 2000). It is known that the total PDI cross section peaks at $h\nu \sim 102$ eV (Samson *et al* 1998 and references therein) and table 1 shows that most of the previous measurements have been made below this maximum. The region above $h\nu \sim 102$ eV is also of interest, as here the cross section starts decreasing and a different regime for the PDI process might significantly change the angular distributions. Only the total PDI cross section (or its ratio to single ionisation) has been extensively studied in this region (see Samson *et al* 1998); TDCS measurements are scarce and remain a challenge due to both the diminishing cross section and the increasing energy phase space. As most spectrometers have a low-energy detection limit, high photon energies also provide the opportunity to reach large values of the energy asymmetry, R .

The measurements were obtained using a dual toroidal coincidence photoelectron spectrometer described in detail elsewhere (Reddish *et al* 1997). Linearly polarised light from an undulator beamline (SU6: $S_1 = 0.9$, $S_3 = 0$, tilt angle (λ) = 0° , $\mathbf{DE}_{FWHM} \sim 700$ meV) at the Super-ACO synchrotron was employed. Photons from the exit slit of the monochromator interact with an effusive beam of helium atoms. The gas enters the chamber through a cylindrically symmetric conical nozzle that surrounds the photon beam. This system, which employs a near-coaxial geometry for the photon and atom sources, is based on the design of

Kämmerling and Schmidt (1993). The precise geometry of the interaction region is therefore different from the previous 40 eV study (Cvejanoviæ *et al* 2000) where the gas was admitted through a hypodermic needle mounted orthogonally to the photon beam direction. The new design has the advantage of cylindrical symmetry around the axis of the toroidal analysers, thus minimising possible systematic errors arising from the geometry of the interaction region. Unfortunately, it has the disadvantage of increasing the metal surface area near the interaction region, which in turn increases the noise due to secondary electrons; this is reflected in the statistical quality of the results. Subsequent refinement of the coaxial gas source design is described in Seccombe *et al* (2001). Electrons emitted in the plane perpendicular to the photon beam direction were detected in coincidence by two independent toroidal analysers with useful angular ranges of $\sim 60^\circ$ and $\sim 140^\circ$. The energy-dependent angular responses of the individual analysers were calibrated using \mathbf{b} values associated with the $\text{He} \rightarrow \text{He}^+ N=2$ transition, based on a fit to the measurements of Wehlitz *et al* (1993) ($\mathbf{b} = 0.30, 0.57, 1.20, 1.48$ and 1.53 for 5, 10, 30, 50 and 55 eV, respectively). The energy resolutions, ΔE_{FWHM} , for the two toroidal analysers were chosen to be ~ 600 meV for E_1 or $E_2 \geq 30$ eV and ~ 300 meV for $E_1 < 30$ eV. The values for S_l and λ were determined from comparative measurements of the single ionisation angular distributions for $\text{He}^+ N=1$ and 2. For reasons of statistical accuracy and clarity of presentation, the analysed data from the continuous angular ranges of the two detectors were ‘binned’ into 10° -wide sectors. This procedure does not significantly alter the shapes of the measured mutual angle distributions.

Helium TDCSs measured for the equal energy sharing condition ($E_1 = E_2 = 30$ eV) are shown in figure 1. Each individual plot represents the TDCS at the given value of \mathbf{q}_l ; the \mathbf{q}_2 distributions reproduce the expected two-lobe structure. The two curves through the data have been calculated in the velocity gauge using the 3C and CCC theories; in both cases the TDCSs determined in the length gauge were virtually the same. The 3C theory and the experimental data points are normalised to the CCC theory at $\mathbf{q}_l = 90^\circ$ as the TDCSs are largest here and exhibit a symmetric profile. For all values of \mathbf{q}_l the CCC theory shows good agreement with the experimental data. As \mathbf{q}_l departs from 90° however, the 3C theory progressively underestimates the width of the larger of the two lobes. This observation is different from the 40 eV excess energy case where the CCC and 3C TDCS shapes were practically indistinguishable. Returning to equation 1, the ungerade amplitude (a_u) is necessarily zero for equal energy sharing, and consequently this situation is relatively straightforward to parametrise since only the gerade amplitude is required. The equal energy data in figure 1 was fitted to equation (2) ($S_l = 0.9$, $S_3 = 0$) using the Levenberg-Marquardt algorithm with a_g represented by the Gaussian ansatz:

$$a_g(E_1, E_2, \mathbf{q}_{l2}) = A \exp\left(\frac{-2 \ln 2 (\mathbf{q}_{l2} - \mathbf{p})^2}{\Gamma^2}\right) \quad (5)$$

with \mathbf{G} denoting the half-width of $|a_g|^2$. The best fit yields a value of $109 \pm 2^\circ$ ($\pm 1\sigma$ statistical fluctuation) for \mathbf{G} (A was determined to an accuracy of $\sim 5\%$), which is to be compared with $103 \pm 2^\circ$ at 40 eV above threshold (Cvejanoviæ *et al* 2000). Kheifets and Bray (2000) have presented values for \mathbf{G} from a number of experiments along with those determined by CCC theory. Our new value shows excellent agreement with their CCC prediction (110°) and fits the trend of the earlier experimental results. We should note, however, that a physical justification for employing equation (5) to represent a_g has only been established in the PDI threshold region where \mathbf{G} and a_g are simply a function of E and are independent of R . Hence, its use at such a high excess energies is questionable. This being said the fits obtained for $E_l =$

E_2 using Gaussian functions are generally very good even for energies well in excess of threshold. For a more detailed discussion of this surprising feature see Kheifets and Bray (2000), Cvejanovi  and Reddish (2000), and Briggs and Schmidt (2000). The present results extend this property up to 60 eV. More precise data, however, including lower values of q_{12} , may reveal deviations from the simple Gaussian shape.

TDCSs measured for the energy-sharing conditions $R = 5$ ($E_1 = 10$ eV, $E_2 = 50$ eV) and 11 ($E_1 = 5$ eV and $E_2 = 55$ eV) are shown in figures 2 and 3 for $q_1 = 0^\circ, 10^\circ, 20^\circ$ and 30° . For both R values, the toroidal analyser with the smaller angular range was used to detect the slower electron. For unequal energy sharing conditions there is no node for back-to-back emission except when $q_1 = 90^\circ$ (see (1)). A three lobe structure is anticipated for all values of q_1 shown and is most evident when $q_1 = 0^\circ$, where there will also be mirror symmetry about the polarisation axis. Our measurements have a limited range of q_2 , but using a procedure based on the symmetry properties of the TDCS (for full description see Cvejanovi  *et al* 2000) we were able to extend the q_2 range for $q_1 = 10^\circ$ and 20° to include all three lobes. The four measured TDCSs at each R are fully inter-normalised assuming the coincident overlap to be independent of the mutual angles; we estimate an upper limit to the inter-normalisation error of $\sim 10\%$. The four curves through each of the data sets in figures 2 and 3 are the result of 3C and CCC calculations in both the length (L) and velocity (V) gauges. A brief description of the details of the calculations is given in our previous paper (Cvejanovi  *et al* 2000). All theoretical TDCSs are normalised to the CCC(V) theory at $q_1 = 90^\circ$. Due to the fact that no experimental measurements were made at $\theta_1 = 90^\circ$, the data sets were arbitrarily normalised.

For $R = 5$, the TDCSs calculated by the 3C theory exhibit a significant gauge dependence; a similar observation was made at 40 eV (Cvejanovi  *et al* 2000) and the general issue of the 3C gauge sensitivity has been discussed by Lucey *et al* (1993). For example, at $q_1 = 0^\circ$ the 3C(V) ‘opposite-to-side’ lobe ratio is $\sim 30\%$ larger than that calculated using 3C(L). In contrast the CCC theory appears to be relatively insensitive to the gauge with only small discrepancies in both shape and magnitude being evident. In general the experimental data agree more closely with the CCC and 3C(L) TDCSs than those determined using 3C(V), whilst at 40 eV excess energy the measured TDCSs generally lie between those determined by the two 3C gauges normalised in the same manner. Discarding the 3C(V) calculations, which have poor agreement, there are still noticeable differences between theory and experiment. Experimentally, the TDCS is smallest near $q_1 = 0^\circ$ and therefore difficult to measure accurately. Theoretically, this may reflect the fact that at these q_1 angles close to the electric field vector, the angular factors in (1) greatly enhance the relative contribution of the ungrade term in the transition amplitude, which is otherwise much smaller than that of the grade term. When the contributions of the two terms of different symmetry (in (1)) are of similar magnitude, the ‘interference’ term is maximised and, for these electron energies, this has a dramatic effect on the shape of the mutual angle distribution.

In the $R = 11$ situation, the 3C TDCSs are more gauge sensitive than is the case for $R = 5$ (see figure 3). For example, at $q_1 = 0^\circ$, the 3C(V) ‘opposite-to-side’ lobe ratio is $\sim 60\%$ larger than that calculated using 3C(L). Again, the CCC calculations exhibit no significant gauge dependence. As with $R = 5$, the experimental data agree more closely with the CCC and 3C(L) TDCSs than those determined using the 3C(V). Moreover, the agreement between the CCC theory and experiment for both $R = 5$ and 11 is generally better here than that reported at 40 eV above threshold (Cvejanovi  *et al* 2000). On theoretical grounds alone, this could be indicative that the CCC method is inherently more reliable at higher excess energies. The size

of the basis set required for convergence as a function of R and excess energy has been discussed in Kheifets and Bray (2000), who state that CCC calculations are more difficult for equal energy sharing conditions, particularly near threshold. It should be noted that the present CCC calculations were performed using a larger basis set ($l_{max} = 5$ as compared to $l_{max} = 4$) than at 40 eV.

The present data can be compared with the pioneering TDCS measurement by Schwarzkopf *et al* (1994) obtained with $E_1 = 5\text{eV}$, $E_2 = 47.9\text{eV}$ at $\mathbf{q}_I = 0^\circ$ and with $S_I = 0.99$. Their study first demonstrated the ‘classic’ three-lobe structure of the He TDCS with asymmetric kinematic conditions. Although it is limited to one \mathbf{q}_I value, the statistical quality of the Schwarzkopf *et al* (1994) data, together with the clear symmetry of their measured profile, is superior to this work. Despite the similarity in excess energy, a direct comparison of their experimental results with those of this study is not entirely straightforward due to the significant differences in S_I and R . Consequently, it is more informative to compare the relative agreement with theory. In Schwarzkopf *et al* (1994), the TDCS measurement was compared with the 3C(V) theory. Maulbetsch and Briggs (1994) demonstrated that the TDCS shape gave best agreement, in terms of the opposite-to-side lobe ratio, with the data using the velocity form of the 3C method. It is interesting to note, therefore, that in this work it is the 3C(L) form that is closest in shape to both the experiment and the CCC theory for $R = 5, 11$, and that once normalised to CCC at 90° , its relative magnitude evolves with \mathbf{q}_I consistently with CCC. This is most evident for $R = 5$ (see Figure 2), and less so for $R = 11$ (see Figure 3) where the CCC method has significantly more yield for small values of \mathbf{q}_{I2} . Clearly, large excess energies and R -values, along with small mutual angles, show the largest discrepancies amongst the theoretical approaches. Unfortunately, these are the most challenging experimental conditions and further work here is clearly needed.

For unequal energy-sharing conditions the ungerade amplitude is only negligible when the excitation energy approaches the PDI threshold. Hence to fit unequal energy-sharing data, functional forms for both a_g and a_u are required. Malegat *et al* (1997a) have derived a general parametrisation for the two amplitudes based on bipolar harmonics. However, there are a large number of parameters involved and hence its application to the present data (and much of the previously published data) would result in significant ambiguities arising from non-unique fits. Cvejanoviæ and Reddish (2000) introduced a ‘practical’ parametrisation adopting Gaussian functions to approximate both amplitudes and have shown that good fits can be obtained with as few as three adjustable parameters. The merit of this approach is that, from the fitted parameters of each E and R data set, one can predict the general TDCS shape over the whole range of emission angles and Stokes parameters. The application of this parametrisation to the current data is not presented here, as it will be included in another study.

To summarise, the spectra presented here have a similar form to those reported previously at 40 eV above threshold (Cvejanoviæ *et al* 2000), showing no sign of radically different regime of electron interactions over that energy span. Comparison with theories shows that they are generally in good agreement with CCC calculations. Under unequal energy-sharing conditions the 3C theory is too gauge dependent to be considered reliable at this excess energy, although it yields the correct features in the TDCS - especially in the length form. In the future, it is hoped that the results of this work will also be compared with the HRM-SOW theory of Malegat *et al* (2000) and other emerging methods.

Acknowledgements

This work was funded by EPSRC, the EU Large Scale Facilities Fund, and LSAI. SC thanks the Leverhulme Trust for his fellowship; CD thanks Newcastle University for a studentship; DPS and FM thank EPSRC for their PDRA positions. We would also like to acknowledge the valuable contribution of N. Dubuisson during the synchrotron beamtime period.

References

- Achler M, Mergel V, Spielberger L, Dörner R, Azuma Y and Schmidt-Böcking H 2001 *J. Phys. B: At. Mol. Opt. Phys.* **34** 965
- Bolognesi P, Camilloni R, Coreno M, Turri G, Berakdar J, Kheifets A, and Avaldi L, 2001, submitted to *J. Phys. B: At. Mol. Opt. Phys.*
- Bräuning H *et al* 1998 *J. Phys. B: At. Mol. Opt. Phys.* **31** 5149
- Briggs J S and Schmidt V 2000 *J. Phys. B: At. Mol. Opt. Phys.* **33** R1
- Collins S A, Huetz A, Reddish T J, Seccombe D P and Soejima K 2001 submitted to *Phys. Rev. Lett*
- Cvejanoviæ S, Wightman J P, Reddish T J, Maulbetsch F, MacDonald M A, Kheifets A S and Bray I 2000 *J. Phys. B: At. Mol. Opt. Phys.* **33** 265
- Cvejanoviæ S and Reddish TJ 2000 *J. Phys. B: At. Mol. Opt. Phys.* **33** 4691
- Dawber G, Avaldi L, McConkey A G, Rojas H, MacDonald M A and King G C 1995 *J. Phys. B: At. Mol. Opt. Phys.* **28** L271
- Dörner R *et al* 1998 *Phys. Rev. A* **57** 1074
- Huetz A and Mazeau J 2000 *Phys. Rev. Lett.* **85** 530
- Huetz A, Lablanquie P, Andriæ L, Selles P and Mazeau J 1994 *J. Phys. B: At. Mol. Opt. Phys.* **27** L13
- Huetz A, Selles P, Waymel D and Mazeau J 1991 *J. Phys. B: At. Mol. Opt. Phys.* **24** 1917
- Kämmerling B and Schmidt V 1993 *J. Phys. B: At. Mol. Opt. Phys.* **26** 1141
- Kazansky A K and Ostrovsky V N 1994 *J. Phys. B: At. Mol. Opt. Phys.* **27** 447
- 1995 *J. Phys. B: At. Mol. Opt. Phys.* **28** 1453
- Kheifets A S, Bray I, Soejima K, Danjo A, Okuno K and Yagishita A 1999 *J. Phys. B: At. Mol. Opt. Phys.* **32** 1501
- Kheifets A S and Bray I 1998a *Phys. Rev. A* **57** 2590
- 1998b *J. Phys. B: At. Mol. Opt. Phys.* **31** L447
- 1998c *Phys. Rev. A* **58** 4501
- 1998d *Phys. Rev. Lett.* **81** 4588
- 2000 *Phys. Rev. A* **62** 065402
- Lablanquie P, Mazeau J, Andriæ L, Selles P and Huetz A 1995 *Phys. Rev. Lett.* **74** 2192
- Lucey S P, Rasch J, Whelan C T and Walters H R J 1998 *J. Phys. B.* **31** 1237
- Malegat L, Selles P and Huetz A 1997a *J. Phys. B: At. Mol. Opt. Phys.* **30** 251
- Malegat L, Selles P, Lablanquie P, Mazeau J and Huetz A 1997b *J. Phys. B: At. Mol. Opt. Phys.* **30** 263
- Malegat L, Kazansky A K and Selles P 1999a *J. Phys. IV* **9** 85
- 1999b *J. Phys. B: At. Mol. Opt. Phys.* **32** 4667
- Malegat L, Selles P and Kazansky A K 1999c *Phys. Rev. A* **60** 3667
- 2000 *Phys. Rev. Lett.* **85** 4450
- Maulbetsch F and Briggs J S 1993a *J. Phys. B: At. Mol. Opt. Phys.* **26** 1679
- 1993b *J. Phys. B: At. Mol. Opt. Phys.* **26** L647
- 1994 *J. Phys. B: At. Mol. Opt. Phys.* **27** 4095
- Maulbetsch F, Pont M, Briggs J S and Shakeshaft R 1995 *J. Phys. B: At. Mol. Opt. Phys.* **28**

L341

- Mazeau J, Andric L, Jean A, Lablanquie P, Selles P and Huetz A 1996 *Atomic and Molecular Photoionization* ed. A Yagishita and T Sasaki (Tokyo: Universal Academy) pp 31 - 8
- Mergel V *et al* 1998 *Phys. Rev. Lett.* **70** 5301
- Pindzola M S and Robicheaux F J 2000 *Phys. Rev. A* **61** 052707
- Pont M and Shakeshaft R 1995 *Phys. Rev. A* **51** R2676
- Pont M, Shakeshaft R, Maulbetsch F and J S Briggs 1996 *Phys. Rev. A* **53** 5671
- Proulx D and Shakeshaft R 1993 *Phys. Rev. A* **48** R875
- Reddish T J, Richmond G, Bagley G W, Wightman J P and Cvejanoviæ S 1997 *Rev. Sci. Instrum.* **68** 2685
- Samson J A R, Stolte W C, He Z X, Cutler J N, Lu Y and Bartlett R J 1998 *Phys. Rev. A* **57** 1906
- Schwarzkopf O, Krässig B, Elmiger J and Schmidt V 1993a *Phys. Rev. Lett.* **70** 3008
- Schwarzkopf O, Krässig B and Schmidt V 1993b *J. Phys. IV* **3** 169
- Schwarzkopf O, Krässig B, Schmidt V, Maulbetsch F and Briggs J S 1994 *J. Phys. B: At. Mol. Opt. Phys.* **27** L347
- Schwarzkopf O and Schmidt V 1995 *J. Phys. B: At. Mol. Opt. Phys.* **28** 2847
- Seccombe D P, Collins S A and Reddish T J 2001, *Rev. Sci. Instrum.* **72** 2550
- Soejima K, Danjo A, Okuno K and Yagishita A 1999 *Phys. Rev. Lett.* **83** 1546
- Viefhaus J, Avaldi L, Heiser F, Hentges R, Gessner O, Rüdél A, Wiedenhöft M, Wieliczek K and Becker U 1996a *J. Phys. B: At. Mol. Opt. Phys.* **29** L729
- Viefhaus J *et al* 1996b *Phys. Rev. Lett.* **77** 3975
- Wehlitz R, Langer B, Berrah N, Whithfield S B, Viefhaus J and Becker U 1993 *J. Phys. B: At. Mol. Opt. Phys.* **26** L783
- Wightman J P, Cvejanoviæ S and Reddish TJ 1998 *J. Phys. B: At. Mol. Opt. Phys.* **31** 1753

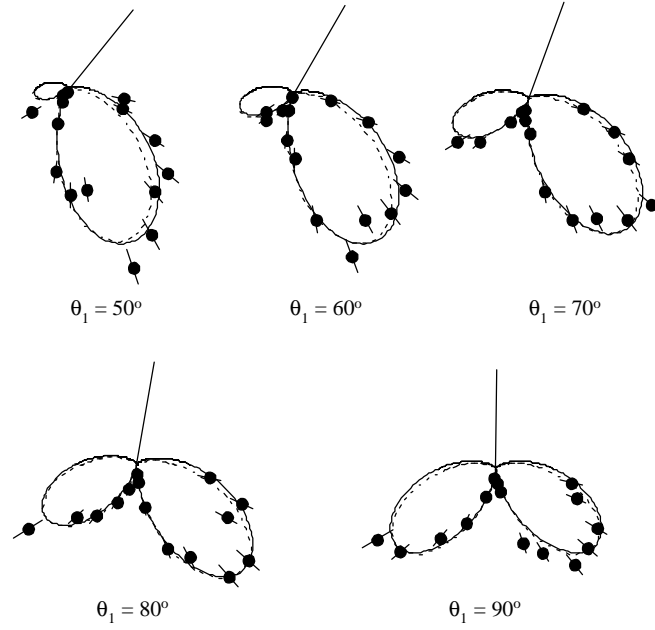


Figure 1. Five TDCSs with $E_1 = E_2 = 30$ eV measured simultaneously and compared with the CCC (solid curve) and 3C (dotted curve) calculations, both in the velocity gauge. The 3C theory and the data set are scaled to the CCC TDCS at $q_I = 90^\circ$, as discussed in the text. The cross section scale is indicated by the length of the line depicting the orientation of the first electron with respect to the polarisation direction, and is equal to $2.75 \cdot 10^{-24} \text{cm}^2 \text{eV}^{-1} \text{sr}^{-2}$. The CCC SDCS equals 0.145 kb eV^{-1} .

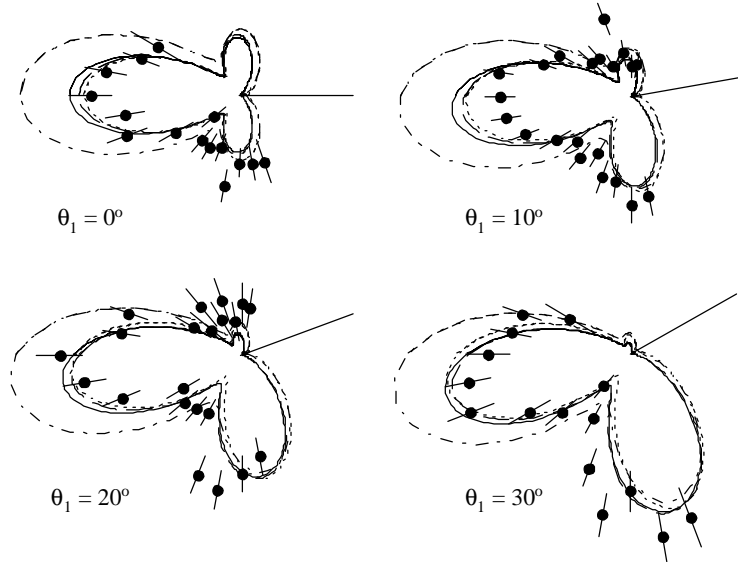


Figure 2. TDCS in He at an excess energy of 60 eV for $E_I = 10$ eV. The CCC calculations (velocity - full line, length -dashed) provide the absolute scale, indicated by the length of the straight line showing the direction of the fixed angle electron ($= 3.8 \cdot 10^{-24} \text{cm}^2 \text{eV}^{-1} \text{sr}^{-2}$). The CCC SDCS equals 0.202 kb eV^{-1} . The 3C calculation in both gauges (velocity - dash-dot, length - dotted) are re-scaled to the CCC(V) result for $q_I = 90^\circ$, as discussed in the text. The experimental data set is arbitrarily normalised.

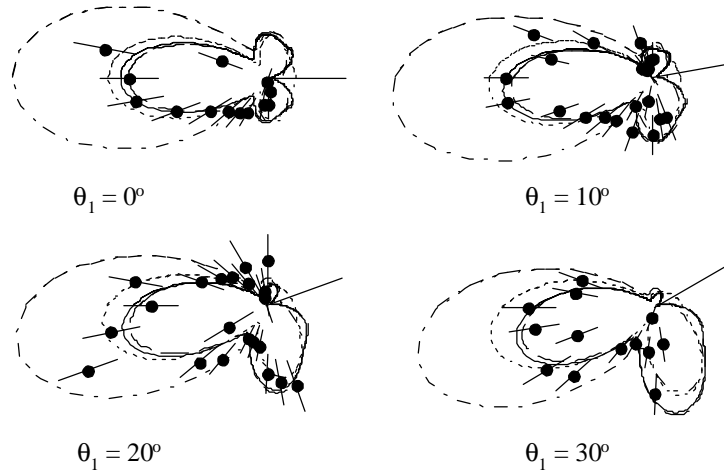


Figure 3. TDCS in He at an excess energy of 60 eV for $E_I = 5$ eV. The CCC calculations (velocity - full line, length -dashed) provide the absolute scale, indicated by the length of the straight line showing the direction of the fixed angle electron ($= 4.4 \cdot 10^{-24} \text{ cm}^2 \text{ eV}^{-1} \text{ sr}^{-2}$). The CCC SDCS equals 0.230 kb eV^{-1} . The 3C calculation in both gauges (velocity - dash-dot, length - dotted) are re-scaled to the CCC(V) result for $q_I = 90^\circ$, as discussed in the text. The experimental data set is arbitrarily normalised.

Table 1. Previous helium TDCS measurements, excluding those probing the effects of circular dichroism.

Excess Energy (E) / eV	Energy Asymmetry $R = E_2 / E_1$	Study
0.1	Unselected	Huetz and Mazeau (2000)*
0.2	Unselected	Huetz and Mazeau (2000)*
0.6	0.3, 1, 3	Dawber <i>et al</i> (1995)
1	1, 5.7	Dawber <i>et al</i> (1995)
	1	Dörner <i>et al</i> (1998)*
2	0.08, 1, 12.3	Dawber <i>et al</i> (1995)
4	1	Huetz <i>et al</i> (1994)
	0.2, 1, 4.7	Lablanquie <i>et al</i> (1995)
	0.2, 1, 4.7	Mazeau <i>et al</i> (1996)
6	0.11, 1, 9	Dörner <i>et al</i> (1998)*
10	1	Schwarzkopf <i>et al</i> (1993b)
17.6	1	Huetz <i>et al</i> (1994)
18.6	0.2, 1, 5.2	Lablanquie <i>et al</i> (1995)
	0.12, 1, 8.3	Mazeau <i>et al</i> (1996)
20	1	Schwarzkopf <i>et al</i> (1993a, b)
	1	Schwarzkopf and Schmidt (1995)*
	0.11, 1, 9	Dörner <i>et al</i> (1998)*
	0.025, 0.053, 0.176, 0.25, 1, 1.86, 4, 5.67, 20, 40	Bräuning <i>et al</i> (1998)*
	1	Wightman <i>et al</i> (1998)
25	4	Collins <i>et al</i> (2001)
40	1, 3, 7	Cvejanoviæ <i>et al</i> (2000)
	0.14, 7	Bolognesi <i>et al</i> (2001)
52.9	9.6	Schwarzkopf <i>et al</i> (1994)
15-51	R - Distribution	Viefhaus <i>et al</i> (1996a)

* Absolute measurements